Nonlinear Buckling Optimization of Composite Structures

Lindgaard, Esben; Lund, Erik

Published in:
Computer Methods in Applied Mechanics and Engineering

DOI (link to publication from Publisher):
10.1016/j.cma.2010.02.005

Publication date:
2010

Document Version
Accepted author manuscript, peer reviewed version

Nonlinear Buckling Optimization of Composite Structures

Esben Lindgaard*, Erik Lund*

Department of Mechanical Engineering, Aalborg University, Pontoppidanstraede 101, DK-9220 Aalborg East, Denmark

Abstract

The paper presents an approach to nonlinear buckling fiber angle optimization of laminated composite shell structures. The approach accounts for the geometrically nonlinear behaviour of the structure by utilizing response analysis up until the critical point. Sensitivity information is obtained efficiently by an estimated critical load factor at a precritical state. In the optimization formulation, which is formulated as a mathematical programming problem and solved using gradient-based techniques, a number of the lowest buckling factors is included such that the risk of "mode switching" during optimization is avoided. The presented optimization formulation is compared to the traditional linear buckling formulation and two numerical examples, including a large laminated composite wind turbine main spar, clearly illustrate the pitfalls of the traditional formulation and the advantage and potential of the presented approach.

Keywords: Composite laminate optimization, Buckling, Design sensitivity analysis, Geometrically nonlinear, Composite structures

1. Introduction

The use of fibre-reinforced polymers has gained an ever-increasing popularity due to their superior mechanical properties. Designing structures made out of composite material represents a challenging task, since both thicknesses, number of plies in the laminate and their relative orientation must be selected. The best use of the capabilities of the material can only be gained through a careful selection of the layup. This work focuses on optimal design of laminated composite shell structures i.e. the optimal fiber orientations within the laminate which is a complicated problem. One of the most significant advances of optimal design of laminate composites is the ability of tailoring the material to meet particular structural requirements with little waste of material capability. Perfect tailoring of a composite material yields only the stiffness and strength required in each direction. A survey of optimal design of laminated plates and shells can be found in [1].

Stability is one of the most important objectives/constraints in structural optimization and this also holds for many laminated composite structures, e.g. a wind turbine blade. Traditionally in optimization, stability is regarded as the linear buckling load, but for structures exhibiting a nonlinear response when loaded the traditional approach can lead to unreliable design results, see e.g. [2]. In stability analysis the buckling load is often approximated by linearized eigenvalue analysis at an initial prebuckling point (linear buckling analysis) and the buckling load is generally overestimated. In the case where nonlinear effects cannot be ignored nonlinear path tracing analysis is necessary. For limit point instability, several standard finite element procedures allow the nonlinear equilibrium path to be traced until a point just before the limit point. The traditional Newton like methods will probably fail in the vicinity of the limit point and the post-critical path cannot be traced. More sophisticated techniques, as the arc-length methods suggested by [3] and subsequently modified by [4] and [5] are among some of the techniques available today for path tracing analysis in the post-buckling regime.

A more accurate estimate of the buckling load, than that obtainable with linear buckling, can be obtained by performing a geometrically nonlinear response analysis and approximate the buckling load by an eigenvalue analysis on the deformed configuration. Various eigenvalue problems have been suggested for the stability analysis of nonlinear structures. [6] and [7] formulated linear eigenvalue problems with information at one load step on the nonlinear prebuckling path. This formulation is referred as the "one-point" approach, where stiffness information is extrapolated until a singular tangent stiffness is obtained. [8] formulated a linear eigenvalue problem utilizing tangent information at two successive load steps on the nonlinear prebuckling path, and are referred as the "two-point" approach.

Optimization with stability constraints has been studied extensively in the past. [9] and [10] described an optimality criterion method for determining the minimum weight design of linear space truss structures subjected to stability constraints. They solved linear stability analysis problems to obtain the critical load and obtained sensitivities by differentiating the discretized matrix eigenvalue problem with respect to design variables. Later methods for obtaining optimum designs of truss

☆Postprint version, final version available at https://doi.org/10.1016/j.cma.2010.02.005

*Correspondence to: Department of Materials and Production, Aalborg University (AAU), Fibigerstræde 16, 9220 Aalborg East, Denmark. Corresponding author E-mail address: elo@mp.aau.dk

Email addresses: elo@me.aau.dk (Esben Lindgaard), el@me.aau.dk (Erik Lund)

structures with stability constraints while considering geometric nonlinearities were presented by [11] by using a relation based on equal strain energy density in all members.

[12] presented design sensitivities of the buckling load for nonlinear structures by taking derivatives of discretized matrix equations with respect to design variables. The method only works for limit points and the critical point needs to be precisely determined for evaluation of sensitivities. [13] presented a variation of the formula that would not only work for limit points but also for bifurcation points.

[14] presented a formulation of continuum design sensitivity analysis of the critical load based on the "one-point" and "two-point" linearized eigenvalue problem. Their expressions would work at any prebuckling point on the nonlinear equilibrium path. They noted that the design sensitivities did not converge to those of the exact critical load when approximated in the near vicinity of the critical point due to divergence in the derivatives of the displacements.

[15] approximated the exact design sensitivities derived by [12] by applying the concept from nonlinear stability analysis, either by "one-point" or "two-point" approach. It was noted that the approximated design sensitivities converged to those by [12] when the approximation point approaches the exact critical point. [16] adopted the method by [15] and included imperfections for avoidance of bifurcation points.

Research on the subject of structural optimization of composite structures considering stability has been reported by many investigators. The first work to appear concerned simple composite laminated plates and circular cylindrical shells where stability was determined by solution of buckling differential equations, see [17, 18, 19, 20, 21, 22, 23, 24, 25, 26]. Later, buckling optimization of composite structures was considered in a finite element framework where the buckling load was determined by the solution to the linearized discretized matrix eigenvalue problem at an initial prebuckling point. Optimization of laminated composite plates has been studied by [27, 28, 29, 30, 31, 32], while others considered more complex composite structures as curved shell panels and circular cylindrical shells, see [33, 34, 35, 36, 37, 38, 39, 40]. However, applications of optimization methods to stability analysis and design of a general type of complex laminated composite shell structures have been very limited. To the best knowledge of the authors only one paper reports on nonlinear gradient based buckling optimization of composite laminated plates and shells, namely the paper by [41], where limit load optimization is considered.

Another important topic in structural stability is the study of the influence of initial imperfections. Imperfections are deviations from the perfect structure, i.e. the analysis model, and can in general be geometrical, structural, material or load related. Despite initial imperfections may be important in terms of the stability load of a structure it is not considered in the present paper.

This paper presents an integrated and reliable method for doing optimization of composite structures w.r.t. stability by including the nonlinear response by a path tracing analysis, here by the arc-length method, in the optimization formulation using the Total Lagrangian formulation. The nonlinear path tracing analysis is stopped when a limit point is encountered and the critical load is approximated at a precritical load step according to the "one-point" approach. Design sensitivities of the critical load factor are obtained semi-analytically by the direct differentiation approach on the approximate eigenvalue problem described by discretized finite element matrix equations. A number of the lowest buckling load factors are considered in the optimization formulation in order to avoid problems related to "mode switching" well-knowing that issues may be encountered due to divergence of the displacement sensitivities. The proposed method is benchmarked against a formulation based on linear buckling analysis on two engineering examples of laminated composite structures. This will help clarify the importance of the nonlinearity in structural design optimization w.r.t. stability.

In this work only Continuous Fiber Angle Optimization (CFAO) is considered thus fiber orientations in laminate layers with preselected thickness and material are chosen as design variables in the laminate optimization.

The "traditional" linear formulation for buckling analysis, sensitivity analysis and optimization formulation is outlined in Section 2 and 3. In Section 4 the proposed procedure regarding nonlinear buckling analysis is stated. Derivations of design sensitivities, using the direct differentiation approach, of the nonlinear buckling load are presented along with the nonlinear buckling optimization formulation in Section 5. Both methods are benchmarked upon engineering examples of laminated composite structures. In Section 6 a laminated composite U-profile is studied while a much more complicated structure of a generic main spar of a wind turbine blade is studied in Section 7. Conclusions are outlined in Section 8.

2. Linear Buckling Analysis of Laminated Composite Shell Structures

The finite element method is used for determining the linear buckling load factor of the laminated composite structure, thus the derivations are given in a finite element context.

A laminated composite is typically composed of multiple materials and multiple layers, and the shell structures can in general be curved or doubly-curved. The materials used in this work are fiber reinforced polymers, e.g. Glass or Carbon Fiber Reinforced Polymers (GFRP/CFRP), oriented at a given angle θ_k for the k^{th} layer or softer isotropic core material. All materials are assumed to behave linearly elastic and the structural behaviour of the laminate is described using an equivalent single layer theory where the layers are assumed to be perfectly bonded together such that displacements and strains will be continuous across the thickness.

The solid shell elements used for all the examples in this paper are derived using a continuum mechanics approach so the laminate is modelled with a geometric thickness in three dimensions, see [42]. The element used is an eight node isoparametric element where shear locking and trapezoidal locking are avoided by using the concepts of assumed natural strains (ANS) for, respectively, out-of-plane shear interpolation, see [43], and

through-the-thickness interpolation, see [44]. Membrane and thickness locking is avoided by using the concepts of enhanced assumed strains (EAS) for the interpolation of the membrane and thickness strains, respectively, see [45, 44]. The EAS interpolation is used to enhance the compatible strain tensor with an independent incompatible strain tensor, and the solid shell element used has seven internal degrees of freedom for the representation of the enhanced strains. This is the lowest number of internal degrees of freedom to introduce for the enhanced strains if the element should pass the in-plane membrane and out-of-plane bending patch tests, see [46] for details.

The static equilibrium equation for the structure may be written as

$$\mathbf{K}_0\mathbf{D} = \mathbf{R} \tag{1}$$

Here $\mathbf{D}$ is the global displacement vector, $\mathbf{K}_0$ is the global initial stiffness matrix, and $\mathbf{R}$ the global load vector.

Based on the displacement field, obtained by the solution to (1), the element layer stresses can be computed, whereby the stress stiffening effects due to mechanical loading can be evaluated by computing the initial stress stiffness matrix $\mathbf{K}_\sigma$. By assuming the structure to be perfect with no geometric imperfections, stresses are proportional to the loads, i.e. stress stiffness depends linearly on the load, displacements at the critical/buckling configuration are small, and the load is independent of the displacements, the linear buckling problem can be established as

$$\left(\mathbf{K}_0 + \lambda_j \mathbf{K}_\sigma\right)\boldsymbol{\phi}_j = \mathbf{0}, \qquad j = 1, 2, \ldots, J \tag{2}$$

where the eigenvalues are ordered by magnitude, such that λ_1 is the lowest eigenvalue, i.e. buckling load factor, and $\boldsymbol{\phi}_1$ is the corresponding eigenvector i.e. buckling mode. In general, for engineering shell structures, the eigenvalue problem in (2) can be difficult to solve, due to the size of the matrices involved and large gaps between the distinct eigenvalues. For efficient and robust solutions, (2) is solved by a subspace method with automatic shifting strategy, Gram-Schmidt orthogonalization, and the sub-problem is solved by the Jacobi iterations method, see [47].

Most often in engineering classical linear buckling analysis is used as a generalized stability predictor for shell structures as described in [48]. For some cases, despite whether the critical point is a bifurcation or limit point, the classical theory yields a satisfactory prediction of the collapse load while it in other cases gives results of little or no value. Despite that it beforehand is unknown whether the classical theory gives satisfactory predictions of the collapse load of a general shell structure it is often used. Since the structures analyzed with linear buckling analysis are perfect with no imperfections of any kind together with the assumptions involved in the theory, the prediction will typically be an upper limit for the real collapse load, and the method is therefore in literature often stated as non-conservative in an engineering context, see e.g. [49].

3. Design Sensitivity Analysis and Optimization of the Linear Buckling Problem

The objective of the work is, by use of gradient-based techniques, to maximize the lowest buckling load factors, and thus the buckling load factor sensitivities should be computed in an efficient way. Only derivations upon structural finite element discretized simple eigenvalues are presented in this paper. In case of non-unique eigenvalues, i.e. multiple eigenvalues, the sensitivity analysis is more complicated due to the non-differentiability of the eigenvalues. In such situations the sensitivity analysis described in [50] may be used.

3.1. Design sensitivity analysis of simple eigenvalues

The eigenvalue problem considered in (2) is a generalized eigenvalue problem of the form

$$\mathbf{K}\boldsymbol{\phi}_j = \lambda_j \mathbf{M}\boldsymbol{\phi}_j, \quad j = 1, 2, \ldots, J \tag{3}$$

It is assumed that the eigenvectors are $\mathbf{M}$-orthonormalized, i.e. $\boldsymbol{\phi}_j^T \mathbf{M}\boldsymbol{\phi}_j = 1$. This means that $\boldsymbol{\phi}_j^T(-\mathbf{K}_\sigma)\boldsymbol{\phi}_j = 1$. In order to obtain the eigenvalue sensitivities, (2) is differentiated with respect to any design variable, $a_i, i = 1, \ldots, I$, assuming that λ_j is simple.

$$\frac{d\lambda_j}{da_i}(-\mathbf{K}_\sigma)\boldsymbol{\phi}_j = \left(\frac{d\mathbf{K_0}}{da_i} - \lambda_j\frac{d(-\mathbf{K}_\sigma)}{da_i}\right)\boldsymbol{\phi}_j + \left(\mathbf{K_0} - \lambda_j(-\mathbf{K}_\sigma)\right)\frac{d\boldsymbol{\phi}_j}{da_i} \tag{4}$$

By premultiplying by $\boldsymbol{\phi}_j^T$, make use of the $\mathbf{M}$-orthonormality of the eigenvectors, (2), and noting that the system matrices are symmetric, the following expression is obtained for the eigenvalue sensitivity.

$$\frac{d\lambda_j}{da_i} = \boldsymbol{\phi}_j^T\left(\frac{d\mathbf{K_0}}{da_i} + \lambda_j\frac{d\mathbf{K}_\sigma}{da_i}\right)\boldsymbol{\phi}_j \tag{5}$$

In order to determine the linear buckling sensitivity $\frac{d\lambda_j}{da_i}$ for any of the design variables a_i, $i = 1, \ldots, I$, the derivative of the element initial stiffness matrix and the derivative of the element stress stiffness matrix have to be derived. These derivatives are determined semi-analytically at the element level by finite difference approximations and assembled to global matrix derivatives.

$$\frac{d\mathbf{k}_0}{da_i} \approx \frac{\mathbf{k_0}(a_i + \Delta a_i) - \mathbf{k_0}(a_i - \Delta a_i)}{2\Delta a_i} \tag{6}$$

$$\frac{d\mathbf{K_0}}{da_i} = \sum_{n=1}^{N_e^{as}}\frac{d\mathbf{k_0}}{da_i}, \quad i = 1, \ldots, I \tag{7}$$

$\mathbf{k_0}$ is the element initial stiffness matrix, Δa_i is the design perturbation, and N_e^{as} is the number of elements in the finite element model associated to the design variable a_i.

The stress stiffness matrix is an implicit function of the displacement field, i.e. $\mathbf{K}_\sigma = \mathbf{K}_\sigma(\mathbf{D}(\mathbf{a}), \mathbf{a})$, which must be considered

$$\frac{d\mathbf{K}_\sigma}{da_i} = \frac{\partial\mathbf{K}_\sigma}{\partial a_i} + \frac{\partial\mathbf{K}_\sigma}{\partial\mathbf{D}}\frac{d\mathbf{D}}{da_i} \tag{8}$$

The displacement sensitivities $\frac{d\mathbf{D}}{da_i}$ must be computed, which is done by direct differentiation of the static equilibrium equation, see (1), w.r.t. a design variable a_i, $i = 1, \ldots, I$.

$$\mathbf{K_0}\frac{d\mathbf{D}}{da_i} = -\frac{d\mathbf{K_0}}{da_i}\mathbf{D} + \frac{d\mathbf{R}}{da_i}, \quad i = 1, \ldots, I \tag{9}$$

The displacement sensitivity $\frac{d\mathbf{D}}{da_i}$ can be evaluated by backsubstitution of the factored global initial stiffness matrix in (9). The initial stiffness matrix has already been factored when solving the static problem in (1) and can here be reused, whereby only the new terms on the right hand side of (9), called the pseudo load vector, need to be calculated. Note that the force vector derivatives, $\frac{d\mathbf{R}}{da_i}$, are zero for design independent loads as in the case for CFAO. The global initial stiffness matrix derivative $\frac{d\mathbf{K_0}}{da_i}$ were determined in (7).
The stress stiffness sensitivity $\frac{d\mathbf{K}_\sigma}{da_i}$ is not evaluated by (8) since it requires partial derivatives of the stress stiffness matrix with respect to displacements, $\frac{\partial \mathbf{K}_\sigma}{\partial \mathbf{D}}$, which is not trivial. Instead it is computed by central difference approximations at the element level for all elements for each design variable a_i, $i = 1, \ldots, I$.

$$\frac{d\mathbf{k}_\sigma}{da_i} \approx \frac{\mathbf{k}_\sigma(a_i + \Delta a_i, \mathbf{D} + \Delta\mathbf{D}) - \mathbf{k}_\sigma(a_i - \Delta a_i, \mathbf{D} - \Delta\mathbf{D})}{2\Delta a_i} \tag{10}$$

The displacement increment is estimated as $\Delta\mathbf{D} \approx \frac{d\mathbf{D}}{da_i}\Delta a_i$, where the displacement sensitivity, $\frac{d\mathbf{D}}{da_i}$, is obtained by solving (9).

3.2. The mathematical programming problem

The optimization problem is in essence a max-min problem where the objective is to maximize the lowest buckling load factor. A direct formulation of the optimization problem can give problems related to differentiability and fluctuations during the optimization process due to "mode switching" (crossing eigenvalues). These problems are circumvented by the use of the socalled bound formulation, see [51] and [52].

$$\begin{aligned}
\text{Objective :} \quad & \max_{\boldsymbol{a},\beta} \ \beta \\
\text{Subject to :} \quad & \lambda_j \geq \beta, \quad j = 1, \ldots, N_\lambda \\
& \left(\mathbf{K_0} + \lambda_j \mathbf{K}_\sigma\right)\boldsymbol{\phi}_j = \mathbf{0} \\
& \underline{a_i} \leq a_i \leq \overline{a_i}, \quad i = 1, \ldots, I
\end{aligned}$$

where a_i denote the design variables in terms of fiber angles. The bound β is introduced, both as a new artificial variable and objective function. The previous non-differentiable objective function, for the max-min problem, is, via the bound formulation, transformed into a set of N_λ constraints.

The mathematical programming problem is solved by the Method of Moving Asymptotes (MMA) by [53]. The closed loop of analysis, design sensitivity analysis and optimization is repeated until convergence in the design variables or until the maximum number of allowable iterations has been reached.

4. Nonlinear Buckling Analysis of Laminated Composite Shell Structures

In order to perform structural stability optimization it is crucial to have a robust and precise objective function at its disposal. Thus, it is desired to determine a more precise objective in terms of instability from which design sensitivities for employment in design optimization can be derived. Structural stability/buckling is now estimated in terms of geometrically nonlinear analyses and restricted to limit point instability, despite that the presented formulas also works well for bifurcation points. In addition, bifurcation instability are in many cases transformed into limit point instability with the introduction of small disturbances/imperfections to the system. The proposed procedure for nonlinear buckling analysis, considering limit points, is schematically shown in Fig. 1 and consists of the steps stated in Algorithm 1.

Algorithm 1 Pseudo code for the nonlinear buckling analysis

1: Geometrically nonlinear (GNL) analysis by arc-length method
2: Monitor and detect limit point during GNL analysis
3: Re-set all state variables to configuration at load step just before limit point
4: Perform eigenbuckling analysis on deformed configuration at load step before limit point

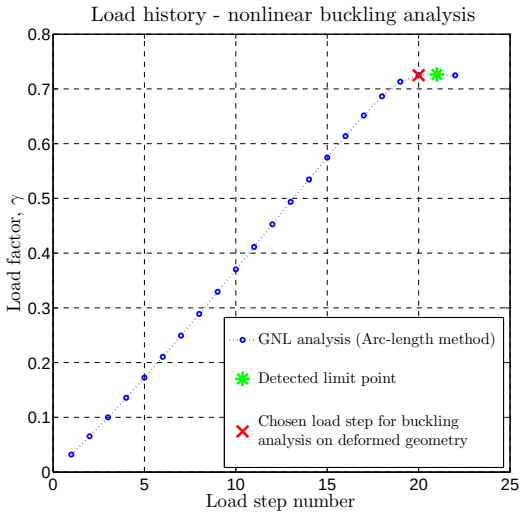

Figure 1: Detection of limit load in step 2.

The limit load in step 2 is simply defined by monitoring the load factor in the GNL analysis. When the load factor from two successive load steps decreases the previous converged load factor is defined as the limit load, see Fig. 1.

Let us consider geometrically nonlinear behaviour of structures made of linear elastic materials. We adopt the Total Lagrangian approach, i.e. displacements refer to the initial configuration, for the description of geometric nonlinearity. An incremental formulation is more suitable for nonlinear problems and it is assumed that the equilibrium at load step n is known and

it is desired at load step $n+1$. Furthermore, it is assumed that the current load is independent on deformation. The incremental equilibrium equation in the Total Lagrangian formulation is written as (see e.g. [6, 54])

$$\mathbf{K_T}(\mathbf{D}^n, \gamma^n)\,\delta\mathbf{D} = \mathbf{R}^{n+1} - \mathbf{F}^n \tag{11}$$

$$\text{where} \quad \mathbf{K_T}(\mathbf{D}^n, \gamma^n) = \mathbf{K_0} + \mathbf{K_L}(\mathbf{D}^n, \gamma^n) + \mathbf{K}_\sigma(\mathbf{D}^n, \gamma^n) \tag{12}$$

$$\text{i.e.} \quad \mathbf{K}_\mathbf{T}^n = \mathbf{K_0} + \mathbf{K}_\mathbf{L}^n + \mathbf{K}_\sigma^n \tag{13}$$

Here $\delta\mathbf{D}$ is the incremental global displacement vector, $\mathbf{F}^n$ global internal force vector, and $\mathbf{R}^{n+1}$ global applied load vector. The global tangent stiffness $\mathbf{K}_\mathbf{T}^n$ consists of the global initial stiffness $\mathbf{K_0}$, the global stress stiffness $\mathbf{K}_\sigma^n$, and the global displacement stiffness $\mathbf{K}_\mathbf{L}^n$. The applied load vector $\mathbf{R}^n$ is controlled by the stage control parameter (load factor) γ^n according to an applied reference load vector $\mathbf{R}$

$$\mathbf{R}^n = \gamma^n\,\mathbf{R} \tag{14}$$

The incremental equilibrium equation (11) is solved by the arc-length method after [5]. During the nonlinear path tracing analysis we can at some converged load step estimate an upcoming critical point, i.e. bifurcation or limit point, by utilizing tangent information. At a critical point the tangent operator is singular

$$\mathbf{K_T}(\mathbf{D}^c, \gamma^c)\,\boldsymbol{\phi}_j = \mathbf{0} \tag{15}$$

where the superscript c denotes the critical point and $\boldsymbol{\phi}_j$ the buckling mode. To avoid a direct singularity check of the tangent stiffness matrix, it is easier to utilize tangent information at some converged load step n and extrapolate it to the critical point. The one-point approach only utilizes information at the current step and extrapolates by only one point. The stress stiffness part of the tangent stiffness at the critical point is approximated by extrapolating the nonlinear stress stiffness from the current configuration as a linear function of the load factor γ.

$$\mathbf{K}_\sigma(\mathbf{D}^c, \gamma^c) \approx \lambda\,\mathbf{K}_\sigma(\mathbf{D}^n, \gamma^n) = \lambda\,\mathbf{K}_\sigma^n \tag{16}$$

It is assumed that the part of the tangent stiffness consisting of $\mathbf{K}_\mathbf{L}^n$ and $\mathbf{K_0}$ does not change with additional loading, which holds if the additional displacements are small. The tangent stiffness at the critical point is approximated as

$$\mathbf{K_T}(\mathbf{D}^c, \gamma^c) \approx \mathbf{K_0} + \mathbf{K}_\mathbf{L}^n + \lambda\,\mathbf{K}_\sigma^n \tag{17}$$

and by inserting into (15) we obtain a generalized eigenvalue problem

$$\left(\mathbf{K_0} + \mathbf{K}_\mathbf{L}^n\right)\boldsymbol{\phi}_j = -\lambda_j\,\mathbf{K}_\sigma^n\,\boldsymbol{\phi}_j \tag{18}$$

where the eigenvalues are assumed ordered by magnitude such that λ_1 is the lowest eigenvalue and $\boldsymbol{\phi}_1$ the corresponding eigenvector. The solution to (18) yields the estimate for the critical load factor at load step n as

$$\gamma_j^c = \lambda_j\,\gamma^n \tag{19}$$

If $\lambda_1 < 1$ the first critical point has been passed and in contrary $\lambda_1 > 1$ the critical point is upcoming. The one-point procedure works well for both bifurcation and limit points. The closer the current load step gets to the critical point, the better the approximation becomes, and it converges to the exact result in the limit of the critical load.

5. Design Sensitivity Analysis and Optimization of the Nonlinear Buckling Problem

To accomplish gradient-based optimization of the nonlinear buckling load factors, the nonlinear buckling load factor sensitivities must be derived. Only simple eigenvalues of conservative load systems are considered.

5.1. Design sensitivity analysis of simple eigenvalues

The eigenvalue problem in (18) is a generalized eigenvalue problem of the form shown in (3) where it is assumed that the eigenvectors are $\mathbf{M}$-orthonormalized, i.e. $\boldsymbol{\phi}_j^T\,\mathbf{M}\,\boldsymbol{\phi}_j = 1$. This means that $\boldsymbol{\phi}_j^T\,(-\mathbf{K}_\sigma^n)\,\boldsymbol{\phi}_j = 1$. By direct differentiation, with respect to any design variable, $a_i, i = 1, \ldots, I$, pre-multiplication of $\boldsymbol{\phi}_j^T$, making use of (18) and the $\mathbf{M}$-orthonormality of the eigenvectors, noting that the system matrices are symmetric, and assuming that λ_j is simple we obtain the eigenvalue sensitivities as

$$\frac{d\lambda_j}{da_i} = \boldsymbol{\phi}_j^T\left(\frac{d\mathbf{K_0}}{da_i} + \frac{d\mathbf{K}_\mathbf{L}^n}{da_i} + \lambda_j\frac{d\mathbf{K}_\sigma^n}{da_i}\right)\boldsymbol{\phi}_j \tag{20}$$

In order to determine the eigenvalue sensitivity $\frac{d\lambda_j}{da_i}$ for any of the design variables a_i, $i = 1, \ldots, I$, the derivatives of the element initial stiffness matrix, element displacement stiffness matrix, and the element stress stiffness matrix have to be derived, respectively. These derivatives are determined semi-analytically at the element level by finite difference approximations and assembled to global matrix derivatives. The element initial stiffness matrix derivative is determined as in (6) and (7). Both the stress stiffness matrix and the displacement stiffness matrix are implicit functions of the displacements, i.e. $\mathbf{K}_\sigma^n = \mathbf{K}_\sigma\left(\mathbf{D}^n(\mathbf{a}), \mathbf{a}\right)$ and $\mathbf{K}_\mathbf{L}^n = \mathbf{K_L}\left(\mathbf{D}^n(\mathbf{a}), \mathbf{a}\right)$, which must be considered. In order to evaluate design sensitivities of $\frac{d\mathbf{K}_\mathbf{L}^n}{da_i}$ and $\frac{d\mathbf{K}_\sigma^n}{da_i}$ semi-analytically by finite difference approximations on the element level, see (10), the displacement sensitivities must be computed. At the converged load step n, we can write the equilibrium equation as

$$\mathbf{Q}^n(\mathbf{D}^n(\mathbf{a}), \mathbf{a}) = \mathbf{F}^n - \mathbf{R}^n = \mathbf{0} \tag{21}$$

where $\mathbf{Q}^n(\mathbf{D}^n(\mathbf{a}), \mathbf{a})$ is the socalled residual or force unbalance. Taking the total derivative of this equilibrium equation with respect to any of the design variables $a_i, i = 1, \ldots, I$, we obtain

$$\frac{d\mathbf{Q}^n}{da_i} = \frac{\partial\mathbf{Q}^n}{\partial a_i} + \frac{\partial\mathbf{Q}^n}{\partial\mathbf{D}^n}\frac{d\mathbf{D}^n}{da_i} = \mathbf{0} \tag{22}$$

$$\text{where} \quad \frac{\partial\mathbf{Q}^n}{\partial\mathbf{D}^n} = \frac{\partial\mathbf{F}^n}{\partial\mathbf{D}^n} - \frac{\partial\mathbf{R}^n}{\partial\mathbf{D}^n} \tag{23}$$

$$\text{and} \quad \frac{\partial\mathbf{Q}^n}{\partial a_i} = \frac{\partial\mathbf{F}^n}{\partial a_i} - \frac{\partial\mathbf{R}^n}{\partial a_i} \tag{24}$$

We note that (23) reduces to the tangent stiffness matrix. Since it was assumed that the current load is independent on deformation, $\frac{\partial\mathbf{R}^n}{\partial\mathbf{D}^n} = \mathbf{0}$, we obtain

$$\frac{\partial\mathbf{F}^n}{\partial\mathbf{D}^n} = \mathbf{K}_\mathbf{T}^n \tag{25}$$

By inserting the tangent stiffness and (24) into (22), we obtain the displacement sensitivities $\frac{d\mathbf{D}^n}{da_i}$ as

$$\mathbf{K}_{\mathbf{T}}^n \frac{d\mathbf{D}^n}{da_i} = \frac{\partial \mathbf{R}^n}{\partial a_i} - \frac{\partial \mathbf{F}^n}{\partial a_i} \tag{26}$$

For design independent loads, the term $\frac{\partial \mathbf{R}^n}{\partial a_i} = \mathbf{0}$.
Thus, all terms have been derived for the evaluation of the eigenvalue sensitivities in (20) and the estimate for the nonlinear buckling load factor sensitivity at load step n is

$$\frac{d\gamma_j^c}{da_i} = \frac{d\lambda_j}{da_i}\gamma^n \tag{27}$$

5.2. The mathematical programming problem

The optimization problem of maximizing the lowest of the nonlinear buckling load factors, γ_j^c, is as for the linear case formulated using a bound formulation, see [51], as

$$\begin{aligned}
\text{Objective :} \quad & \max_{\boldsymbol{a},\beta} \ \beta \\
\text{Subject to :} \quad & \gamma_j^c \geq \beta, \quad j = 1,\ldots,N_\lambda \\
& \left(\mathbf{K_0} + \mathbf{K}_{\mathbf{L}}^n + \lambda_j \mathbf{K}_{\boldsymbol{\sigma}}^n\right)\boldsymbol{\phi}_j = \mathbf{0} \\
& \gamma_j^c = \lambda_j \gamma^n \\
& \underline{a_i} \leq a_i \leq \overline{a_i}, \quad i = 1,\ldots,I
\end{aligned}$$

Again, the mathematical programming problem is solved using the Method of Moving Asymptotes by [53]. By utilizing the procedure described in Section 4, the estimation point for the nonlinear buckling analysis and design sensitivity analysis is updated at each optimization iteration, whereby a good approximation of the nonlinear buckling load and sensitivities are obtained since the estimation point always is in the neighbourhood of the real buckling load. As for the linear case, the closed loop of analysis, design sensitivity analysis, and optimization is repeated until convergence in the design variables or until the maximum number of allowable iterations is reached.

6. Numerical Example: Laminated Composite U-Profile

In order to illustrate the importance and the potential of the nonlinear buckling formulation, described in Section 4 and 5, and the pitfalls of the traditional linear buckling formulation, see Section 2 and 3, a laminated composite U-profile is considered. The laminated composite U-profile is an example of a real structural engineering element, e.g. the company *Fiberline Composites A/S* produces such structural elements by a process called pultrusion, see Fig. 2.

Geometry, loading, and boundary conditions are identical to a model analyzed by [45]. The U-profile is clamped at one end and point loaded in an upper corner node at the other end with a force $R = 250kN$. A total of 432 equivalent single layer solid shell finite elements and 962 nodes are used in the numerical model. This model thus has 2808 compatible degrees of freedom and 3024 incompatible degrees of freedom. This

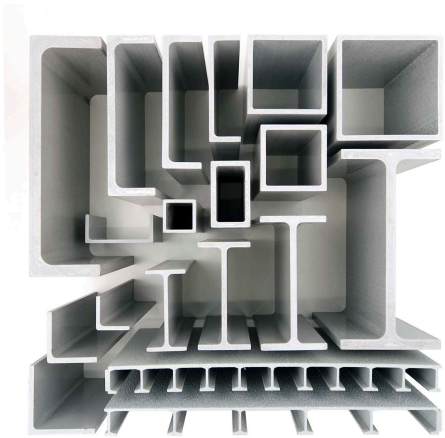

(Courtesy of Fiberline Composites A/S)

Figure 2: Examples of laminated composite profiles manufactured by pultrusion process by the company Fiberline Composites A/S.

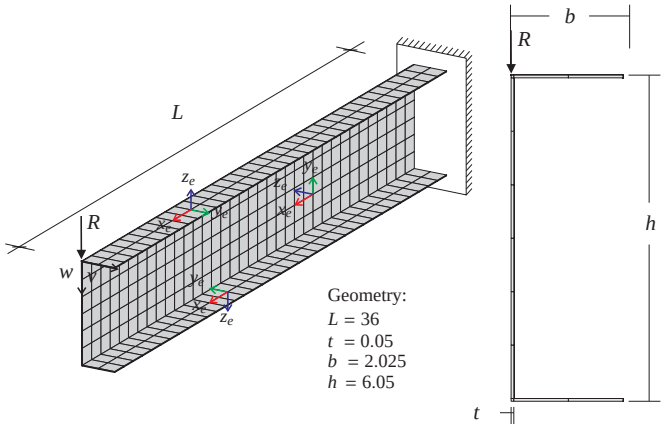

Figure 3: Geometry, loads, boundary conditions, and element coordinate systems for numerical model of the U-profile.

mesh size has been determined through mesh convergence studies and found sufficient for predicting the buckling mode and buckling load. For details about the mesh convergence study see [55]. The laminate layup consists of 4 uni-directional E-glass/epoxy fiber layers each of equal thickness, see properties of the processed material in Table 1.

Table 1: Processed material properties for U-profile.

E-glass/epoxy			
E_x	30.6 GPa	E_y	8.7 GPa
E_z	8.7 GPa	ν_{xy}	0.29
ν_{xz}	0.3	ν_{yz}	0.3
G_{xy}	3.24 GPa	G_{xz}	3.24 GPa
G_{yz}	2.9 GPa	ρ	1686 kg/m^3

The fiber orientation is related to the element coordinate system, (x_e, y_e, z_e), in each finite element. The fiber orientation is measured counterclockwise from the x-axis in the xy-plane of the element coordinate system. The element coordinate system for the finite elements, in respectively the web and each flange, is depicted in Fig. 3. The fiber orientation at each layer in the

web and each flange is considered constant and the layer stacking is done from inside out. Three layup definitions are defined for the U-profile and will be the starting points for the laminate optimization, see Table 2.

Table 2: Layup definitions for the U-profile, which are the starting point for the laminate optimization. Each layer in the laminate layups has a thickness of 12.5*mm*.

Layup 1	
Top Flange	$(-90°, -45°, 0°, 45°)$
Web	$(0°, 45°, 90°, 135°)$
Bottom Flange	$(-45°, 0°, 45°, 90°)$
Layup 2	
Top Flange	$(45°, 0°, -45°, -90°)$
Web	$(135°, 90°, 45°, 0°)$
Bottom Flange	$(90°, 45°, 0°, -45°)$
Layup 3	
Top Flange	$(0°, 45°, -90°, -45°)$
Web	$(90°, 135°, 0°, 45°)$
Bottom Flange	$(45°, 90°, -45°, 0°)$

The representation of the lamina layers for the U-profile is not entirely realistic since the layers preferably should be continuous across the top flange, web, and bottom flange for manufacturing purposes. Alternatively, a continuous lamina layer could be added as the outermost outer layers and act as a binder between the different sections. This issue is not further addressed since the purpose of the numerical example is to demonstrate the different methodologies and not design of a structure ready for manufacturing.

6.1. Structural behaviour of U-profile

Initial analysis is carried out on the U-profile before advanced optimization is proceeded in order to determine the structural behaviour. Only layup 1 in Table 2 is considered. Instability is predicted with linear buckling analysis and geometrically nonlinear path tracing analysis, respectively. Considering geometrically nonlinear analysis as the "exact" prediction, the buckling load predicted by linear buckling analysis is overestimated by 27%, see Fig. 4.

The geometrically nonlinear analysis predicts buckling due to a limit point instability where the structure buckles in the top flange near the fixed support, see Fig. 5. In contrary, linear buckling analysis predicts bifurcation buckling due to collapse in the web section at the free end. Not only does linear buckling overestimate the buckling load, it also fails to predict the buckling shape at the critical point.

6.2. Linear buckling optimization

The laminated composite U-profile is optimized with respect to linear buckling. The fiber angles in the laminate layup definition, see Table 2, are chosen as design variables giving a total of 12 design variables. Since fiber angle optimization is associated with a non-convex design space with many local minima, three different layups/starting points in the design space have been selected for the optimization, see Table 2.

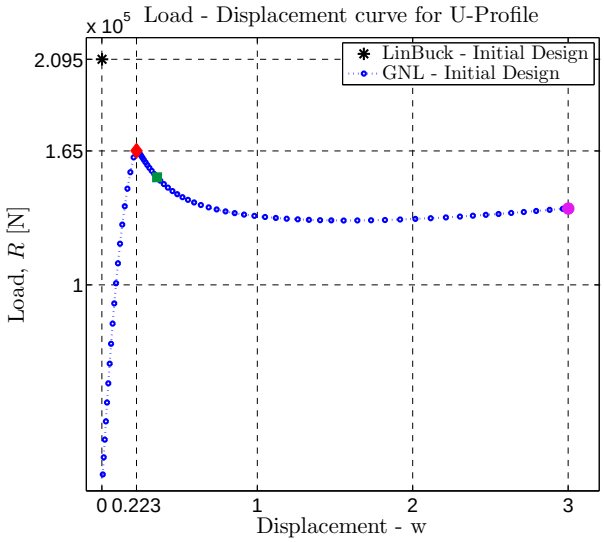

Figure 4: Linear buckling load and load displacement curve from geometrically nonlinear analysis of U-profile with layup 1.

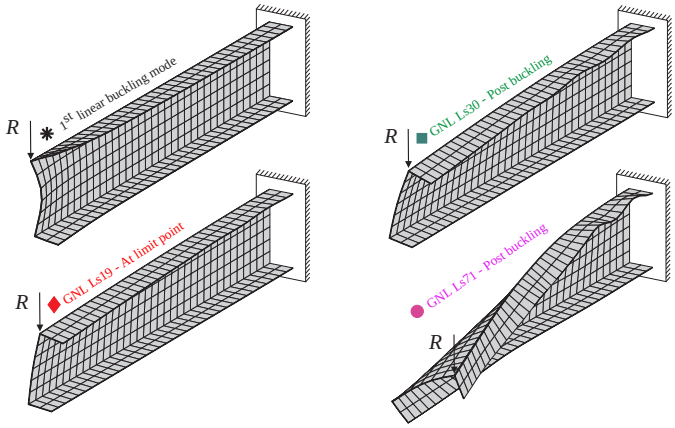

Figure 5: 1st linear buckling mode shape and displacement field at different load steps during the geometrically nonlinear analysis. Note that the displacement fields correspond to the marked load steps on the load displacement curve in Fig. 4.

The linear buckling optimization histories are shown in Fig. 6 for the three starting points and are named LinBuckOpt. LinBuckOpt1 and LinBuckOpt2 converge to the same buckling load while the LinBuckOpt3 converges to a slightly lower linear buckling load.

The optimum fiber angle results from optimization run LinBuckOpt2 is schematically illustrated in Fig. 7. The fiber angles in the flanges are mainly oriented in the length of the U-profile whereas the fiber angles for the web are oriented in the transverse direction in order to suppress the lowest linear buckling mode. Similar fiber angle results in the web are obtained in LinBuckOpt1 and LinBuckOpt3.

In order to validate the results from the linear buckling optimization and to check the effect on the "real" critical load, geometrically nonlinear analyses are carried out for the laminate designs obtained at every 10th iteration during the linear buckling optimization process. The critical load detected at these designs are plotted in Fig. 6. As expected the linear buckling

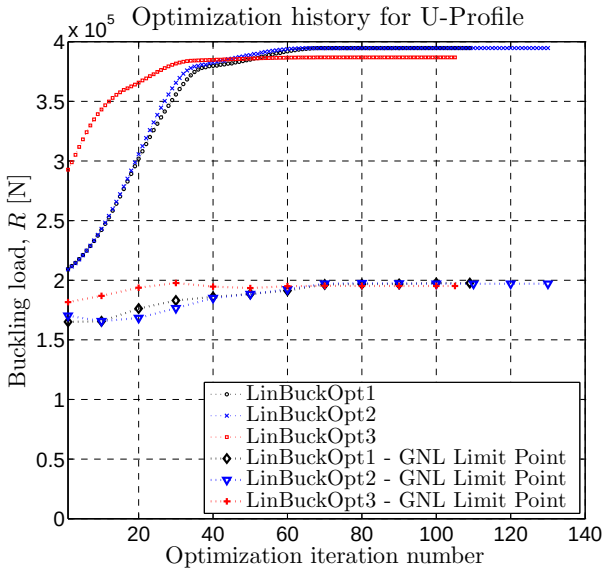

Figure 6: Optimization histories for linear buckling optimization (LinBuckOpt), and detected GNL limit point from re-runned analyses (LinBuckOpt - GNL Limit Point).

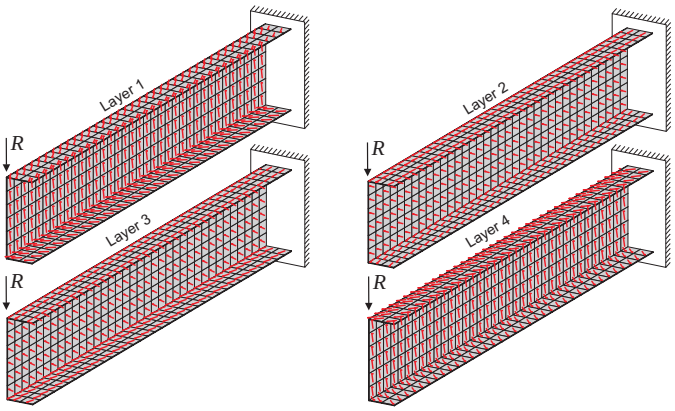

Figure 7: Fiber angle results in all four layers of the U-profile from the linear buckling optimization run LinBuckOpt2.

analysis overestimates the critical load which also was observed in the initial analysis in Section 6.1. But important to notice is that no correlation can be observed between the tendency of the linear buckling load and the real critical load during the optimization. Despite high improvement in the linear buckling load during the optimization only minor gain is achieved in the real critical load. The linear buckling optimization fails to improve the critical load and only the overestimate by linear buckling analysis is maximized.

6.3. Nonlinear buckling optimization

Applying the nonlinear optimization formulation, described in Section 4 and Section 5, the nonlinear buckling load of the composite U-profile is optimized. The same parametrization and starting points as in the linear buckling optimization in Section 6.2 are used. The nonlinear buckling optimization histories are plotted in Fig. 8 and named GNLBuckOpt. Note that the buckling load plotted is the detected limit point during the geometrically nonlinear analysis in the nonlinear buckling optimization procedure, and can therefore be considered as the real critical load.

The nonlinear buckling optimizations, GNLBuckOpt1 and GNLBuckOpt2, attain almost the same buckling load at the final designs. GNLBuckOpt3 gets to a better design with a higher buckling load which demonstrates the risk of ending up in a local minima when using continuous fiber angles as design variables.

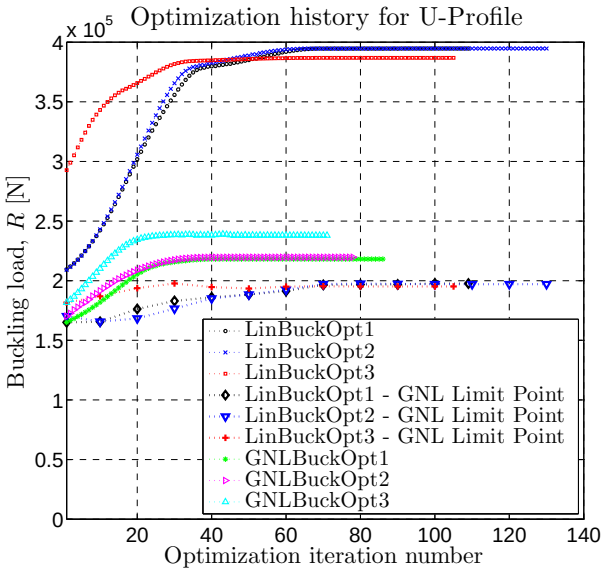

Figure 8: Optimization histories for nonlinear buckling optimization (GNLBuckOpt), linear buckling optimization (LinBuckOpt), and detected GNL limit points from re-runned analyses (LinBuckOpt - GNL Limit Point).

The linear buckling optimization did only yield a limited improvement with respect to the buckling resistance, whereas the nonlinear buckling optimal designs have a considerable improvement in the buckling resistance.

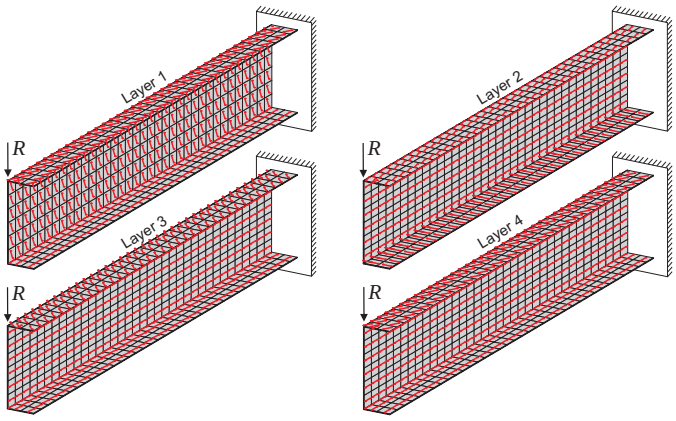

Figure 9: Fiber angle results in all four layers of the U-profile from the nonlinear buckling optimization run GNLBuckOpt3.

The optimal fiber orientation for GNLBuckOpt3 is schematically shown in Fig. 9. Recall that the U-profile buckles near the fixed end in the top flange. At all layers in the top flange the fibers are transversely oriented and closely oriented towards

45°/-45° in order to give resistance against the local buckling mode development. The orientation of the fibers is a tradeoff between global bending stiffness, local suppression of the buckling mode in the top flange, flange width, and a varying moment along the length and width of the top flange which results in large shear near the clamped support. This pinpoints that the use of rational design methods is very beneficial for design of such complicated structures with highly nonlinear behaviour. At the web and the bottom flange the fibers are in most layers oriented in the longitudinal direction for maximum global bending stiffness.

6.4. Comparison

In order to investigate the poor performance of the linear buckling optimized structures w.r.t. the real critical load, see Fig. 8, the linear and nonlinear buckling mode shapes are compared to the post-buckling deformation field from a geometrically nonlinear analysis in Fig. 10. The linear buckling analysis predicts instability in the free end of the web while the U-profile as observed through geometrically nonlinear analysis looses its stiffness due to buckling in the top flange near the fixed support. The nonlinear buckling analysis performed at the deformed configuration near the instability point captures this behaviour. The buckling mode shape is very important in the calculation of accurate design sensitivities since it appears directly in the equations, see (5) and (20). Furthermore, the matrices involved in the buckling problem for both analysis and design sensitivity analysis are more accurate at the updated configuration and the nonlinear buckling optimization formulation proves to be reliable in buckling problems involving large displacements and near limit points.

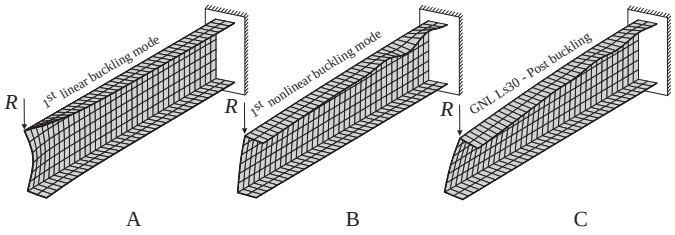

Figure 10: Comparison of buckling mode shapes and displacement field. A: 1st linear buckling mode shape. B: 1st nonlinear buckling mode shape. C: Post-buckling displacement field from geometrically nonlinear analysis.

The linear buckling formulation should be used with caution and not as a general tool to design buckling resistant structures. As depicted in Fig. 8, the real buckling load from the linear buckling optimization runs does not increase monotonously in the first 40 optimization iterations despite the optimization algorithm applied is gradient-based. This indicates a lack of connection between the linear buckling load and the real buckling load. Linear buckling optimization may therefore in some cases not improve the buckling load and maybe even reduce it. Despite misleading high improvement in the linear buckling load during optimization the real buckling load may remain unchanged which for engineering design purposes can be fatal. In case of bifurcation buckling where nonlinear effects cannot be disregarded the nonlinear buckling formulation can still be applied by either introducing imperfections into the structure in order to convert the bifurcation point into a limit point, or by stopping the GNL analysis prior reaching the first bifurcation point. In the latter, the nonlinear buckling analysis and DSA has to be performed at the deformed configuration near the first bifurcation point.

7. Numerical Example: Generic Wind Turbine Main Spar

In order to demonstrate the proposed approach on a more complex structure a generic model of a main spar of a wind turbine blade is studied. The main spar is one of the main carrying components in some designs of wind turbine blades as illustrated in Fig. 11. These designs of wind turbine blades basically consist of two structural components, the main spar and the aerodynamic shell. The main spar is the main carrying structural component for flapwise bending loads whereas the aerodynamic shell carries most of the edgewise bending loads.

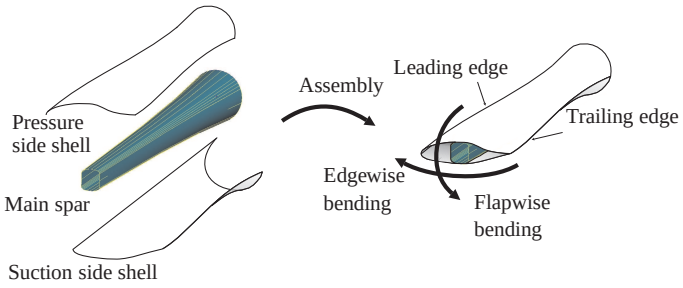

Figure 11: The two main structural components in a typical wind turbine blade design, [56].

In this study the main spar is subjected to the most critical static load case, which is the flapwise bending load that arises when the turbine has been brought to a standstill due to the high wind and the blade is hit by the 50 year extreme wind. With such extreme bending loads the main spar will typically collapse due to local buckling on the compressive side of the blade. According to [57], the ultimate strength of a wind turbine in flapwise bending is characterized by a sequence of failure events where the first is delamination triggered by local buckling and subsequently compressive fibre failure in the main spar.

For the design study of the generic main spar only 14 meter of a 25 meter blade is modelled, see Fig. 12. The finite element model consists of 1856 equivalent single layer solid shell finite elements and 3776 nodes. This model thus has 11136 compatible degrees of freedom and 12992 incompatible degrees of freedom. This mesh size has through mesh convergence studies been found sufficient for analyzing buckling. The resulting flapwise bending load of $R = 164.7kN$ is distributed as a surface load in the tip section (not follower force). The tip section is used for load introduction and the generic main spar model is clamped at the root section. The initial laminate layup of the generic main spar is shown in Fig. 13 and the processed material properties are stated in Table 3.

The root section is a stiff monolithic laminate layup with orientations -10°/10°/10°/-10° and the webs which mainly are

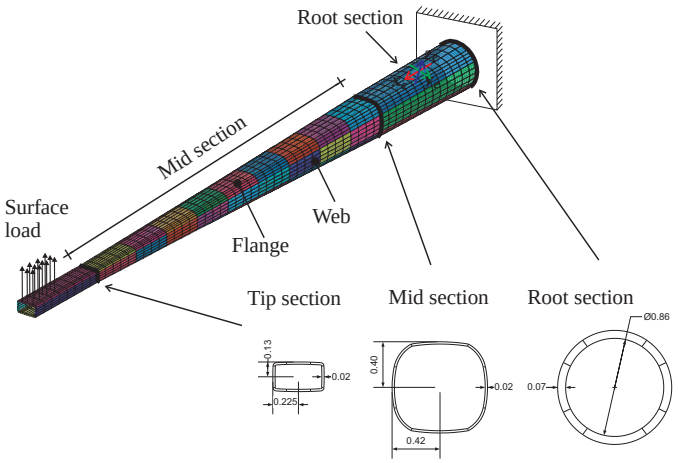

Figure 12: Definition of the generic wind turbine main spar with geometric measures in [m]. It is a generic model without twist of the spar and with a total length of 14 meter. The root section has a length of 3 meter and the mid section which is the design area in the laminate optimization has a length of 9 meter. A linear interpolation between the three cross sections shown is used while the tip section, which is used for load introduction, has a constant cross section. All elements have their element coordinate system, (x_e, y_e, z_e), located such that the x_e-axis is pointing in the longitudinal direction of the main spar and the z_e-axis is pointing outwards.

loaded in shear are made as a sandwich structure with a light foam core material and unidirectional E-glass/epoxy face sheets oriented 45°/-45°. The flanges mainly consist of 0° packs, which involve many 0° layers stacked together for maximum bending stiffness and some 45°/-45° layers for local buckling resistance.

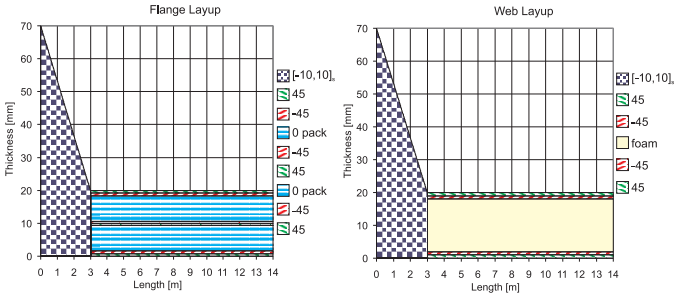

Figure 13: Initial layup definitions for respectively, flanges and webs in the generic main spar model. The layer stacking is done from inside out, i.e. the inner surface of the main spar is at zero thickness.

For real applications the transition between the root layup and the mid section layup, see Fig. 13, will preferable be smooth and not abrupt in order to obtain a smooth stiffness transition and thereby lower the interlaminar effects which may lead to delamination and eventually failure of the blade. Only buckling is considered in this study and the transition did not influence the buckling performance and characteristics whereby the presented layup is considered sufficient in the design study.

7.1. Preliminary analysis of generic main spar

Structural analysis is performed before optimization is proceeded in order to characterize the structural behaviour of the main spar. Both linear buckling analysis and geometrically

Table 3: Processed material properties for the generic main spar.

Material property	E-glass/epoxy (UD)	Foam Rohacell (PMI)
E_x	39.8 GPa	150 MPa
E_y	6.98 GPa	-
E_z	6.98 GPa	-
ν_{xy}	0.298	0.298
ν_{yz}	0.3	-
ν_{xz}	0.298	-
G_{xy}	2.6 GPa	-
G_{xz}	2.6 GPa	-
G_{yz}	2.59 GPa	-
ρ	1900 kg/m^3	110 kg/m^3

nonlinear analysis are utilized to predict the collapse load of the structure. The GNL analysis predicts collapse at a load of 107.2kN in terms of a limit point while linear buckling analysis predicts collapse at a load of 134.7kN. Considering the prediction from GNL analysis as the correct prediction linear buckling analysis overestimates the collapse load by 25.6%. Both analyses predict collapse due to local buckling on the compressive side of the main spar, see Fig. 14.

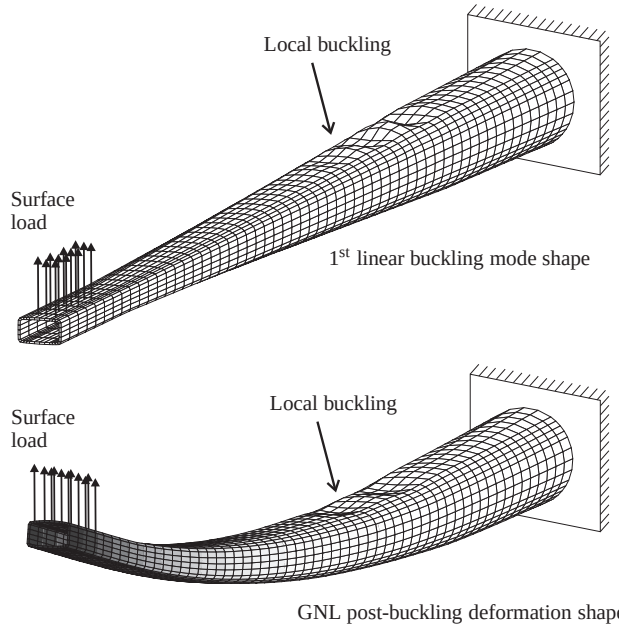

Figure 14: Top: 1st buckling mode shape from linear buckling analysis at a linear buckling load factor of $\lambda_1 = 0.8177$. Bottom: Post-buckled deformation shape from GNL analysis. Critical load factor at the limit point from GNL analysis is $\gamma^c = 0.6510$.

Both analyses with respect to the collapse characteristic of the main spar are in good agreement, i.e. the location of the local buckling is similar, despite the difference in the prediction of the collapse load.

7.2. CFAO of generic main spar

Continuous fiber angle optimization of the generic main spar model is considered where the objective is to maximize the collapse load. Only the biax fiber layers, i.e. the 45° and -45°

layers, are chosen as design variables since these layers are included in the layup of the main spar for improved buckling resistance. The 0° pack layers are excluded in the design optimization whereby the bending stiffness is unaffected by the design changes and a compliance constraint is unnecessary. Only the mid section biax layers for both flanges and webs are considered in the optimization. Patches, covering larger areas of the structure, are introduced. Within a patch containing a set of finite elements only one fiber angle design variable controls the orientation of the given fiber layer in the finite element set. This is a valid approach for practical design problems since laminates are typically made using fiber mats covering larger areas. In the mid section, 1 patch per meter is utilized for both flanges and webs giving a total of 180 fiber angle design variables.

Linear buckling optimization and nonlinear buckling optimization are performed and the optimization histories are collected in Fig. 15. The optimization problems of the generic main spar have been solved on a hybrid Linux cluster "Fyrkat" at Aalborg, Denmark. The programming code which is written in Fortran 95 has been implemented in parallel such that element routines have been parallelized through the use of OpenMP directives, factorization of the global system, (1) and (11), are done in parallel through the Pardiso solver in the Intel Math Kernel Library (MKL), and a Message Passing Interface (MPI) has been incorporated for doing the design sensitivity analysis in parallel.

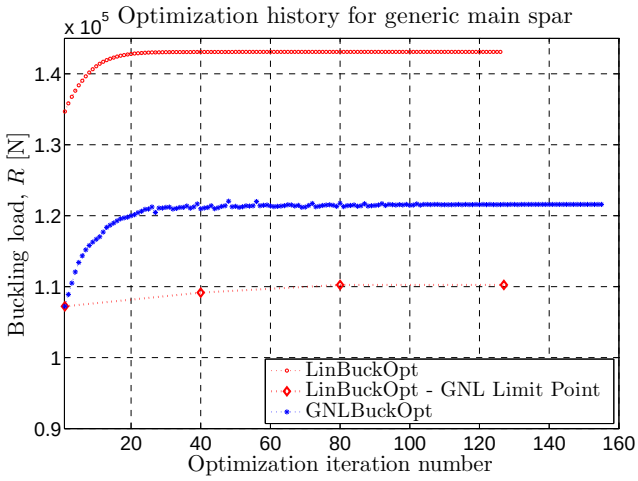

Figure 15: Optimization histories for nonlinear buckling optimization (GNLBuckOpt), linear buckling optimization (LinBuckOpt), and detected GNL limit points from re-runned analyses (LinBuckOpt - GNL Limit Point) of the generic main spar.

The optimization history of the linear buckling load shows considerable improvement while the improvement in the real collapse load in terms of the GNL limit point is limited. The collapse load of the linear buckling optimized design is only 2.8% larger than the collapse load of the initial design. This behaviour was also observed for the U-profile example in Section 6. The nonlinear buckling optimization successfully improves the collapse load of the generic main spar by 13.4%, which in this context is a large improvement considering that only a few biax layers are changed and that the initial layup from an engineering viewpoint is reasonable. The fiber angle results from the nonlinear buckling optimization is depicted in Fig. 16. The fiber angle results from the nonlinear buckling optimization are depicted in Fig. 16. The fiber angles in the area of instability are changed from being 45°/-45° to be more transversely oriented and closely to 90° in order to suppress the local buckling mode and thereby raise the collapse load. Only a few biax layers are selected as design layers and the fixed fiber layers are oriented in the length direction. This choice of parametrization, together with the small effective width compared to the length of the spar, explains the orientation of the design layers in the area of instability. Despite many patch divisions in the parametrization of the problem the fiber angle results are quite continuous across patches which makes manufacturing easier.

Within the optimization of the generic main spar the number of arc-length steps in the vicinity of the limit point has been increased for a better resolution and thereby better limit point detection and easier convergence. This is accomplished by the introduction of a re-initialization feature of the arc-length solver such that the arc-length step is reduced when the load factor is larger than 90% of the detected limit load from the previous optimization iteration. Some small fluctuations are present in the nonlinear buckling optimization history in Fig. 15 which is due to the nonlinearity and non-convexity of the optimization problem. These fluctuations may be avoided by reducing the maximum move limit though increasing the risk of convergence to a local minima.

Many optimization iterations are needed for convergence, see Fig. 15. A convergence criteria based on the relative change of the objective would have resulted in only 20 – 40 optimization iterations, but for completeness a very strict convergence criteria based on the relative design change has been applied.

Despite the linear buckling mode shape and the GNL postbuckling displacement field are quite similar, see Fig. 14, the linear buckling optimization formulation yields very poor results. The is due to the nonlinearity of the problem whereby the design sensitivities for the linear formulation becomes inaccurate since the stress stiffness is not linear together with the missing contribution from the displacement stiffness. The linear formulation is unreliable despite it in the analysis is able to predict the mode of instability and the collapse load within a margin of 25.6% which makes it dangerous for engineering design purposes. Especially in cases where only linear buckling analysis is performed and not even the final result is verified by GNL analysis, the danger of the linear buckling formulation is substantial since the linear buckling optimization shows misleading high improvement of the collapse load while the real collapse load almost remains unchanged.

8. Conclusion

Buckling behaviour of arbitrary composite structures can reliably be improved by the proposed optimization method. The method includes accurate nonlinear path tracing analysis and the buckling load is estimated at a precritical point on the deformed configuration whereby a more precise estimate is ob-

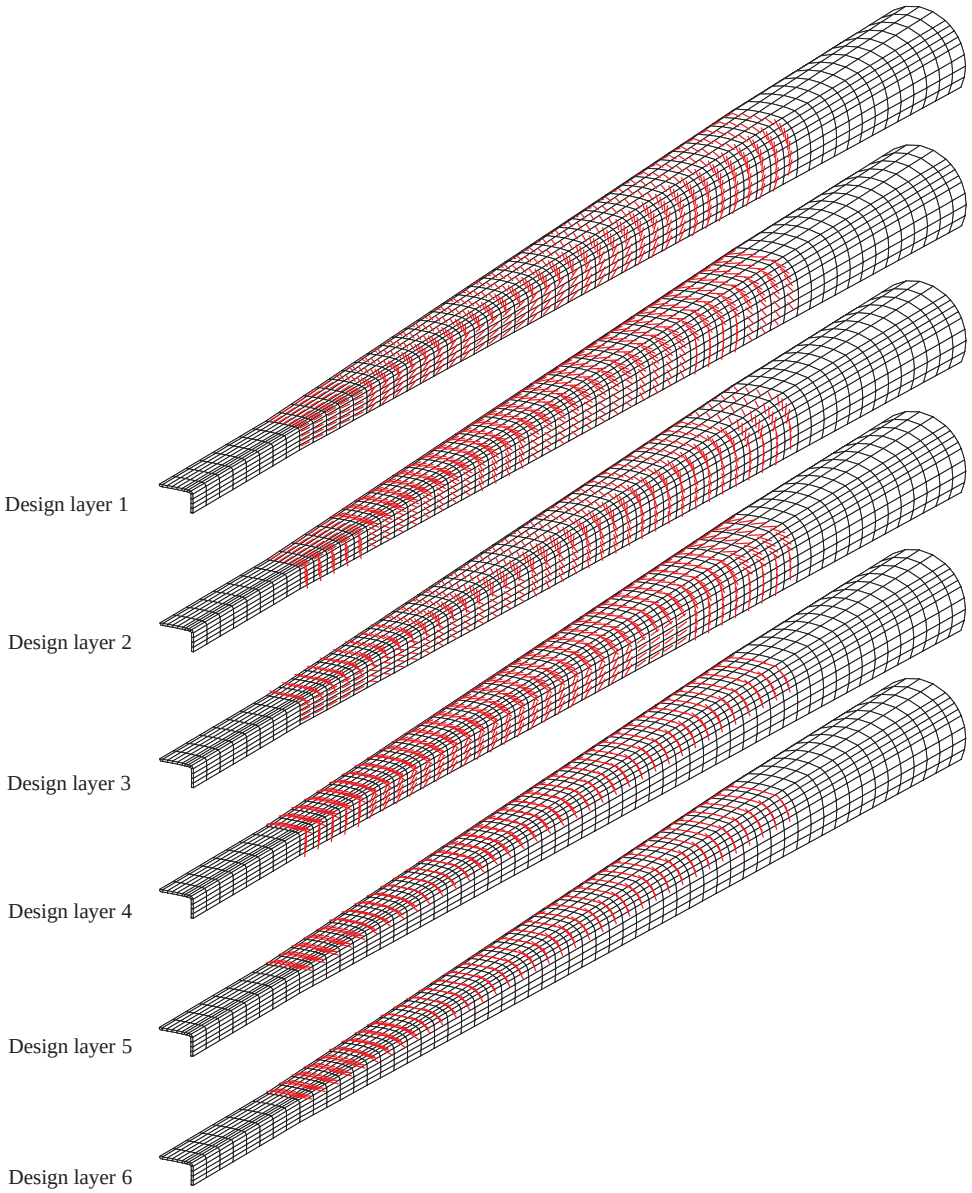

Figure 16: Fiber angle results from nonlinear buckling optimization for half of the generic main spar. Numbering the layer stacking from inside out, design layer 1 contains the first layer for respectively flanges and webs that are chosen as design variables.

tained than that obtainable by classical linear buckling analysis. General sensitivity formulas for the nonlinear buckling load, described by discretized finite element matrix equations, have been derived and the design sensitivities are approximated at the precritical point, thus no exact and troublesome determination of the critical point is necessary.

The current approach is at present limited to a limit point type of instability. It is possible to expand the method to include bifurcation type of instability by modifying the limit point detection in the optimization procedure to a critical point detection that includes both limit points and bifurcation points. During geometrically nonlinear analysis, eigenbuckling analysis could be preformed at some load steps in order to estimate an upcoming critical point, and thereby determine the precritical estimation point for design and design sensitivity analysis of the buckling load.

The method has been applied successfully in the buckling optimization of two composite structures using fiber angle parametrization. The examples demonstrated the importance of the nonlinear buckling formulation and that application of the classical linear buckling formulation may not improve the critical load during the optimization process and as a consequence lead to unreliable design results. Linear buckling analysis is often used to predict instability and to optimize structures for maximum buckling performance without considering nonlinear effects or type of instability. Precautions should be taken before applying the classical linear formulation, especially in cases with nonlinear prebuckling path and in cases with limit point instability. In such cases the nonlinear buckling formulation proves to yield much better results and especially when

the approximation point is close to the critical point. During the benchmarks of the nonlinear formulation good convergence properties was observed and no problems related to divergence of the displacement derivatives could be traced since the estimation point for design sensitivities is located at a precritical state.

Imperfection sensitivity is not considered in the paper but may prove to be important in order to obtain practical estimates of the buckling load. As long as buckling load is used as the objective function, the authors do not expect the effect of imperfection sensitivity to change the optimum designs. This statement is currently being investigated by the authors. On the other hand, if buckling requirements are considered in the form of constraints a detailed analysis of imperfection sensitivity or the use of "engineering" knock-down factors should be used.

Using the developed approach structures can reliably be optimized with respect to a general type stability, i.e. either bifurcation or limit point stability, and especially in cases where geometrically nonlinear effects cannot be ignored. This allows the material utilization of buckling critical laminated structures to be pushed to the limit in an efficient way yet allowing lighter and stronger structures.

Acknowledgements

The authors gratefully acknowledge the support from the Danish Center for Scientific Computing (DCSC) for the hybrid Linux Cluster "Fyrkat" at Aalborg University, Denmark.

[1] S. Abrate, Optimal design of laminated plates and shells, Compos. Struct. 29 (1994) 269–286.
[2] A. Suleman, R. Sedaghati, Benchmark case studies in optimization of geometrically nonlinear structures, Struct. Multidiscip. Optim. 30 (2005) 273–296.
[3] E. Riks, An incremental approach to the solution of snapping and buckling, Int. J. Solids Struct. 15 (1979) 529–551.
[4] E. Ramm, Strategies for tracing nonlinear responses near limit points, in: E. S. W. Wunderlich, K. J. Bathe (Eds.), Nonlinear finite element analysis in structural mechanics, Springer Verlag Berlin Heidelberg New York, 1981, pp. 63–89.
[5] M. A. Crisfield, A fast incremental/iterative solution procedure that handles "snap-through", Compt. Struct. 13 (1981) 55–62.
[6] B. Brendel, E. Ramm, Linear and nonlinear stability analysis of cylindrical shells, Compt. Struct. 12 (1980) 549–558.
[7] C. Borri, H. W. Hufendiek, Geometrically nonlinear behaviour of space beam structures, J. Struct. Mech. 13 (1985) 1–26.
[8] K.-J. Bathe, E. N. Dvorkin, On the automatic solution of nonlinear finite element equations, Compt. Struct. 17 (5-6) (1983) 871–879.
[9] N. S. Khot, V. B. Venkayya, L. Berke, Optimum structural design with stability constraints, Int. J. Numer. Methods Eng. 10 (1976) 1097–1114.
[10] N. S. Khot, Nonlinear analysis of optimized structure with constraints of system stability, AIAA J. 21 (1983) 1181–1186.
[11] N. S. Khot, M. P. Kamat, Minimum weight design of truss structures with geometric nonlinear behaviour, AIAA J. 23 (1985) 139–144.
[12] C. C. Wu, J. S. Arora, Design sensitivity analysis of non-linear buckling load, Comput. Mech. 3 (1988) 129–140.
[13] H. Noguchi, T. Hisada, Sensitivity analysis in post-buckling problems of shell structures, Compt. Struct. 47 (4/5) (1993) 699–710.
[14] J. S. Park, K. K. Choi, Design sensititvity analysis of critical load factor for nonlinear structural systems, Compt. Struct. 36 (5) (1990) 823–838.
[15] T. S. Kwon, B. C. Lee, W. J. Lee, An approximation technique for design sensitivity analysis of the critical load in non-linear structures, Int. J. Numer. Methods Eng. 45 (1999) 1727–1736.
[16] M. Kegl, B. Brank, B. Harl, M. M. Oblak, Efficient handling of stability problems in shell optimization by asymmetric "worst-case" shape imperfection, Int. J. Numer. Methods Eng. 73 (2008) 1197–1216.
[17] G. Sun, J. S. Hansen, Optimal design of laminated-composite circular-cylindrical shells subjected to combined loads, J. Appl. Mech. 55 (1) (1988) 136–142.
[18] A. Muc, Optimal fibre orientation for simply-supported angle-ply plates under biaxial compression, Compos. Struct. 9 (1988) 161–172.
[19] G. Sun, A practical approach to optimal design of laminated cylindrical shells for buckling, Compos. Sci. Technol. 36 (1989) 243–253.
[20] S. Adali, K. J. Duffy, Design of antisymmetric hybrid laminates for maximum buckling load: I. Optimal fibre orientation, Compos. Struct. 14 (1990) 49–60.
[21] K. J. Duffy, S. Adali, Design of antisymmetric hybrid laminates for maximum buckling load: II. Optimal layer thickness, Compos. Struct. 14 (1990) 113–124.
[22] J. L. Grenestedt, Layup optimization against buckling of shear panels, Struct. Optim. 3 (1991) 115–120.
[23] H. Fukunaga, H. Sekine, M. Sato, A. Iino, Buckling design of symmetrically laminated plates using lamination parameters, Compt. Struct. 57 (1995) 643–649.
[24] M. Walker, T. Reiss, S. Adali, Multiobjective design of laminated cylindrical shells for maximum torsional and axial buckling loads, Compt. Struct. 62 (2) (1997) 237–242.
[25] C. G. Diaconu, H. Sekine, Layup optimization for buckling of laminated composite shells with restricted layer angles, AIAA J. 42 (10) (2004) 2153–2163.
[26] S. Honda, Y. Narita, K. Sasaki, Optimization for the buckling loads of laminated composite plates – comparison of various methods, Key Eng. Mater. 334-335 (2007) 89–92.
[27] C. C. Lin, A. J. Yu, Optimum weight design of composite laminated plates, Compt. Struct. 38 (5/6) (1991) 581–587.
[28] M. W. Hyer, H. H. Lee, The use of curvilinear fiber format to improve buckling resistance of composite plates with central circular holes, Compos. Struct. 18 (5/6) (1991) 239–261.
[29] S. B. Biggers, S. Srinivasan, Postbuckling response of piece-wise uniform tailored composite plates in compression, J. Reinf. Plast. Compos. 13 (9) (1994) 803–821.
[30] M. Walker, S. Adali, V. Verijenko, Optimization of symmetric laminates for maximum buckling load including the effects of bending-twisting coupling, Compt. Struct. 58 (2) (1996) 313–319.
[31] M. Walker, Multiobjective design of laminated plates for maximum stability using the finite element method, Compos. Struct. 54 (2001) 389–393.
[32] U. Topal, Ü. Uzman, Maximization of buckling load of laminated composite plates with central circular holes using mfd method, Struct. Multidiscip. Optim. 35 (2008) 131–139. doi:10.1007/s00158-007-0119-1.
[33] H. T. Hu, S. S. Wang, Optimization for buckling resistance of fiber-composite laminate shells with and without cutouts, Compos. Struct. 22 (2) (1992) 3–13.
[34] H. C. Mateus, C. M. M. Soares, C. A. M. Soares, Buckling sensitivity analysis and optimal design of thin laminated structures, Compt. Struct. 64 (1-4) (1997) 461–472.
[35] C. A. Perry, Z. Gürdal, J. H. Starnes, Minimum-weight design of compressively loaded stiffened panels for postbuckling response, Eng. Opt. 28 (1997) 175–197.
[36] J. P. Foldager, J. S. Hansen, N. Olhoff, Optimization of the buckling load for composite structure taking thermal effects into account, Struct. Multidiscip. Optim. 21 (2001) 14–31.
[37] J.-H. Kang, C.-G. Kim, Minimum-weight design of compressively loaded composite plates and stiffened panels for postbuckling strength by genetic algorihtm, Compos. Struct. 69 (2005) 239–246.
[38] H. T. Hu, J. S. Yang, Buckling optimization of laminated cylindrical panels subjected to axial compressive load, Compos. Struct. 81 (2007) 374–385.
[39] E. Lund, Buckling topology optimization of laminated multi-material composite shell structures, Compos. Struct. 91 (2009) 158–167.
[40] U. Topal, Multiobjective optimization of laminated composite cylindrical shells for maximum frequency and buckling load, Mater. Des. 30 (2009) 2584–2594.
[41] J. S. Moita, J. I. Barbosa, C. M. M. Soares, C. A. M. Soares, Sensitivity

analysis and optimal design of geometrically non-linear laminated plates and shells, Compt. Struct. 76 (2000) 407–420.
[42] L. Johansen, E. Lund, J. Kleist, Failure optimization of geometrically linear/nonlinear laminated composite structures using a two-step hierarchical model adaptivity, Compt. Methods Appl. Mech. Engrg. 198 (30-32) (2009) 2421–2438. doi:10.1016/j.cma.2009.02.033.
[43] E. N. Dvorkin, K. J. Bathe, A continuum mechanics based four-node shell element for general non-linear analysis, Eng. Comput. 1 (1984) 77–88.
[44] M. Harnau, K. Schweizerhof, About linear and quadratic "solid-shell" elements at large deformations, Compt. Struct. 80 (9-10) (2002) 805–817.
[45] S. Klinkel, F. Gruttmann, W. Wagner, A continuum based three-dimensional shell element for laminated structures, Compt. Struct. 71 (1) (1999) 43–62.
[46] L. Vu-Quoc, X. G. Tan, Optimal solid shells for non-linear analyses of multilayer composites. I. Statics, Compt. Methods Appl. Mech. Engrg. 192 (9-10) (2003) 975–1016.
[47] E. L. Wilson, T. Itoh, An eigensolution strategy for large systems, Compt. Struct. 16 (1983) 259–265.
[48] B. O. Almroth, F. A. Brogan, Bifurcation buckling as an approximation of the collapse load for general shells, AIAA J. 10 (4) (1972) 463–467.
[49] R. D. Cook, D. S. Malkus, M. E. Plesha, R. J. Witt, Concepts and Applications of Finite Element Analysis, 4th Edition, John Wiley & Sons, Inc., John Wiley & Sons, Inc., 111 River Street, Hoboken, NJ 07030, 2002, ISBN 0-471-35605-0.
[50] A. P. Seyranian, E. Lund, N. Olhoff, Multiple eigenvalues in structural optimization problems, Struct. Optim. 8 (1994) 207–227.
[51] M. P. Bendsøe, N. Olhoff, J. Taylor, A variational formulation for multicriteria structural optimization, J. Struct. Mech. 11 (1983) 523–544.
[52] N. Olhoff, Multicriterion structural optimization via bound formulation and mathematical programming, Struct. Optim. 1 (1989) 11–17.
[53] K. Svanberg, Method of moving asymptotes - a new method for structural optimization, Int. J. Numer. Methods Eng. 24 (1987) 359–373.
[54] E. Hinton (Ed.), NAFEMS Introduction to Nonlinear Finite Element Analysis, Bell and Bain Ltd, Glasgow, 1992, ISBN 1-874376-00-X.
[55] L. S. Johansen, Analysis and optimization of composite structures using adaptive analysis methods, Ph.D. thesis, Department of Mechanical Engineering, Aalborg University, Denmark, special report no. 64 (2009).
[56] L. Kühlmeier, Buckling of wind turbine rotor blades - analysis, design and experimental validation, Ph.D. thesis, Department of Mechanical Engineering, Aalborg University, Denmark, special report no. 58 (2006).
[57] L. C. T. Overgaard, E. Lund, O. T. Thomsen, Structural collapse of a wind turbine blade. Part A: Static test and equivalent single layered models, Submitted.